# Effect of temperature on crystallite size and residual stress of nano-nickel coatings

Shouwen Shen[1*], Jwaher M. Ghamdi[2], Mazen M. Khaled[3], Nayef M. Anazi[4], Ihsan M. Taie[5]

[1,4,5]Research & Development Center, Saudi Aramco, Dhahran, 31311, Saudi Arabia
[2]Chemistry Department, University of Dammam, Dammam, 34212, Saudi Arabia
[3]Chemistry Department, King Fahd University of Petroleum and Minerals, Dhahran, 31261, Saudi Arabia
*Corresponding author; Email: shouwen.shen@aramco.com

***Abstract*—*Nanocrystalline nickel coatings were prepared from a Watts bath using pulse current (PC) condition. To investigate the temperature effect on the crystallite size and residual stress of the nano-nickel coatings, The temperature of the electroplating bath was maintained at 35 °C, 40 °C, 50 °C, 55 °C, and 60 °C respectively. X-ray diffraction (XRD) analysis was performed to determine the crystallite size, relative texture coefficient, and residual stress of the studied coatings. The experimental results show that with increasing temperature of the Watts bath, the average crystallite size, relative texture coefficient of crystallographic plane (200) (same direction as (100)), and compressive residual stress of nanocrystalline nickel coatings increase. It is concluded that moderately increasing the temperature (up to about 60 °C) in the process of nanocrystalline nickel coating production will promote the preferred orientation of crystallographic plane (100) and the compressive residual stress, which enhances nickel crystal compaction, coating adhesion, and coating integrity.*

***Keywords*— Crystallite size, Electro-deposition, Nano-nickel coating, relative texture coefficient, Residual stress, Watts bath temperature.**

## I. INTRODUCTION

The production and characterization of nanocrystalline coatings have been the subjects of intensive research by both the scientific and industrial communities in recent years due to their unique properties conferred by ultrafine crystallite size (typically smaller than 100 nm). There are serveral ways to produce nanocrystalline coatings. Among them, electrodeposition has received considerable attention as a feasible and economically viable technique [1-11]. Research has showed it is important to optimize the electrodeposition conditions of the nanocrystalline nickel coating such as bath temperature, which plays an important role for crystallite size of the electrodeposited coating sample [12-13]. However, very few experiments have been done on the effect of bath temperature on the crystallite size of nickel deposits. In some cases, the reported data are inconsistent or even different. For example, A. M. Rashidi et al [12] explored bath temperature from 45 °C to 65 °C and found that the crystallite size of deposits reduces as the plating temperature increases up to 55 °C and then increases by further increase in the bath temperature. According to Dini [14], it is generally expected that the crystallite size of the deposits increases by increasing the bath temperature and has been experimentally observed for some nanocrystalline deposits. The objective of the present investigation is to further evaluate the influence of bath temperature on the crystallite size, texture, and residual stress of nanocrystalline nickel coatings.

## II. EXPERIMENTAL

Nanocrystalline nickel coatings were prepared from a Watts bath using pulse current (PC) condition. The Watts solution consisted of 280 g/l nickel sulfate hexahydrate and 45 g/l nickel chloride hexahydrate with 45 g/l boric acid (a buffer in the solution). 2 g/l saccharin was added as a grain refiner. The solution was prepared from analytical grade chemicals and deionized water. The pH value of the bath was adjusted to 3.7±0.1 by addition of drops of 10% (wt) HCl and/or 10% (wt) NaOH solutions. The substrate material was carbon steel (C: 0.45%), a 2.5 mm thick strip desk with a diameter of 2.5 cm. Prior to deposition, the steel substrates were mechanically polished with silicon carbide paper of 320, 400, and 600 grits using a Buehler Metaserv grinding/polishing machine until the mirror-like finish was obtained. After that, the substrate desks were rinsed with deionized water and acetone then dried, weighed and placed in the holder which gets 7 $cm^2$ of exposed surface area and 3 cm away from the anode. Electrolytic nickel pellets with 99.9% purity contained in a titanium mesh basket were used as a soluble anode. The temperature of the electroplating bath was maintained at 35 °C, 40 °C, 50 °C, 55 °C, and 60 °C respectively. A Thermo hot plate/stirrer was used for magnetic stirring at 500 rpm. A digital control pulse plating

electric source with square-wave pulse was used for pulse current electroplating techniques. The composition, pulse electroplating parameters and conditions of the electroplating bath are listed in **Table 1**.

**TABLE 1**
**COMPOSITION AND CONDITIONS OF THE ELECTROPLATING BATH**

| | |
|---|---|
| $NiSO_4.6H_2O$ | 280 g/l |
| $NiCl_2.6H_2O$ | 45 g/l |
| $H_3BO_3$ | 45 g/l |
| Saccharine ($C_7H_5NO_3S$) | 2 g/l |
| Temperature | 35, 40, 50, 55 and 60 °C |
| Agitation | magnetic stirrer at 500 rpm |
| pH | 3.7±0.1 |
| Peak current density | 0.35 (A/cm$^2$) |
| Pulse frequency | 100 Hz |
| Duty cycle | 50 % |

The crystallite size, preferred crystallographic orientation, and the residual stress were examined by X-ray diffraction (XRD) technique utilizing a PANalytical X'Pert Pro instrument operated at 45 kV and 40 mA with Cu kα radiation (λ = 1.5418 Å). 0.01° step size and 2 second per step were used for crystallite size determination in the range of 43° to 46° 2θ scan. 0.04° step size and 1.5 second per step were set for relative texture coefficient analysis in the range of 30° to 160° 2θ scan. 0.02° step size and 20 second per step were employed for residual stress analysis in the range of 90.5° to 95.5° of multiple scans at different tilt angles (ψ) of 0°, 21.41°, 31.08°, 39.22°, 46.90°, 54.72°, 63.42°, and 75°.

## III. RESULTS AND DISCUSSION

### 3.1 Crystallite Size

The average crystallite size of the nickel coatings was calculated from XRD patterns using Scherrer's equation given by [15]

$$Dv = k\lambda / \beta \cos\theta \tag{1}$$

Where Dv is the crystallite size weighted by volume, K is the Scherrer constant (somewhat arbitrary varying from 0.62 to 2.08 [15] and depends on crystal shape, usually takes the value of 0.9 as assuming the crystals are spherical with cubic symmetry), λ is the wavelength of X-ray radiation (Å) (if it is Cu X-ray source, then takes 1.5418Å) and β is the integral breadth of peak (in radians 2θ) located at angle θ (usually FWHM (Full Width at Half Maximum) is used for the determination of the integral breadth of peak).

**TABLE 2**
**CRYSTALLITE SIZE CALCULATED FROM XRD SOFTWARE USING DIFFERENT MATHEMATIC MODELS**

| Temperature (°C) | Crystallite Size (nm) | | | | | |
|---|---|---|---|---|---|---|
| | HighScore FWHM | HighScore Integral breadth | Jade 9.1+ Pseudo-Voigt | Jade 9.1+ Pearson VII | Over range | Middle value |
| 35 | 20.9±0.2 | 19.1±0.2 | 19.4±0.2 | 19.8±0.2 | 19.1~20.9 | 20.0 |
| 40 | 22.0±0.2 | 19.7±0.2 | 20.3±0.2 | 20.8±0.2 | 19.7~22.0 | 20.9 |
| 50 | 23.7±0.2 | 21.9±0.2 | 22.0±0.2 | 22.7±0.2 | 21.9~23.7 | 22.8 |
| 55 | 24.8±0.2 | 23.0±0.2 | 23.2±0.2 | 24.0±0.2 | 23.0~24.8 | 23.9 |
| 60 | 28.0±0.3 | 25.9±0.3 | 25.8±0.3 | 26.9±0.3 | 25.8~28.0 | 26.9 |

In the present study, FWHM was utilized for crystallite size calculation. However, there are different methods for FWHM determination, such as FWHM determinations by XRD software HighScore Plus and JADE 9.1$^+$. In which, XRD software JADE 9.1$^+$ method is to perform a XRD pattern profile fitting to calculate FWHM with different mathematic models such as Pseudo-Voigt, Pearson VII, Gaussian, and Lorentzian. In the present work, the reference material of $Y_2O_3$ with average crystal size 30 nm was used for quality control and accuracy check. It was found that the value obtained from our instrument was very close to the actual value of the reference material. The results of crystallite size calculation from different methods using diffraction peak of Ni (111) at 44.4° (2θ) for 5 nickel coatings are shown in **Table 2**. The results show that the values from different methods are similar and the average crystallite size of nickel coatings is in the range between 19 nm and 28 nm.

### 3.2 Relative Texture Coefficient

In order to evaluate the preferred crystallographic orientation of the nickel coatings, the term of relative texture coefficient (RTC(hkl)) was used and defined as[16]:

$$RTC\,(hkl) = \frac{Is\,(hkl)/Ip(hkl)}{\sum_{i=1}^{6} Is\,(hkl)/Ip(hkl)} \times 100\% \quad (2)$$

Where Is(hkl) and Ip(hkl) are the diffraction intensities of the (hkl) plane measured in the diffractogram of the nickel coatings and the standard nickel powder respectively. Only six basic of the total eight diffraction peaks were selected, i.e. (111), (200), (220), (311), (331) and (420), since the diffraction peaks of (222) and (400) are the second-order diffraction of (111) and (200) planes respectively. The term RTC(hkl) expresses the percentage of the relative intensity of a given orientation (hkl) among the six crystallographic orientations of each nickel sample studied, while a preferred orientation of hkl plane is indicated by values of RTC(hkl) ≥ 16.67% [16]. The results of relative texture coefficient (RTC(hkl)) are listed in **Table 3**. It is noted that the crystallographic plane (100) (as the same direction of (200)) has the highest preferred orientation in all samples.

**TABLE 3**
**RELATIVE TEXTURE COEFFICIENT ($RTC_{(HKL)}$) CALCULATED FROM THE SIX BASIC DIFFRACTION PEAKS**

| Temperature (°C) | Relative Texture Coefficient ($RTC_{(hkl)}$) | | | | | | RTC (200) / RTC (111) |
|---|---|---|---|---|---|---|---|
| | (111) | (200) | (220) | (311) | (331) | (420) | |
| 35 | 18.11±0.9 | 25.65±1.3 | 11.82±0.6 | 20.81±1.0 | 11.77±0.6 | 11.84±0.6 | 1.42±0.07 |
| 40 | 25.85±1.3 | 26.74±1.3 | 5.45±0.2 | 26.66±1.3 | 7.25±0.3 | 8.04±0.4 | 1.03±0.05 |
| 50 | 24.77±1.2 | 31.14±1.5 | 3.96±0.2 | 27.63±1.4 | 5.72±0.3 | 6.78±0.3 | 1.26±0.06 |
| 55 | 20.68±1.0 | 34.55±1.7 | 5.49±0.2 | 22.37±1.1 | 8.12±0.4 | 8.79±0.4 | 1.67±0.08 |
| 60 | 20.72±1.0 | 42.89±2.1 | 3.41±0.1 | 21.13±1.0 | 5.94±0.3 | 5.92±0.3 | 2.07±0.10 |

### 3.3 Residual Stress

Knowing the residual stress field in coated components is a primary requirement for their correct design and production. Adhesion, for instance, depends on the residual stress and, in particular, on the residual stress mismatch between coating and substrate. XRD is known to be a valuable technique to measure residual stress in a non-destructive way.

**TABLE 4**
**RESULTS OF RESIDUAL STRESS ANALYSIS**

| Temperature (°C) | Residual Stress (MPa) |
|---|---|
| 35 | -39.3±4.2 |
| 40 | -75.5±5.2 |
| 50 | -86.2±5.9 |
| 55 | -92.5±4.8 |
| 60 | -94.0±5.7 |

In the present study, the $\sin^2\psi$ analysis method [17] was used to measure residual stress of nickel coatings. The residual stress in the coating samples is related to the slope of the plot of strain $\varepsilon = \Delta d/d0$ versus $\sin^2\psi$ using the following equation:

$$\varepsilon = \frac{(1+\nu)\sigma\sin^2\psi}{E} \quad (3)$$

Where E is Young's modulus, ν is the Poisson's ratio and σ is the stress coefficient. The d-spacing measurements were conducted on the high 2θ peak of Ni (311) plane of the coating samples at different tilting (ψ changes at 0°, 21.41°, 31.08°, 39.22°, 46.90°, 54.72°, 63.42°, and 75° respectively). The d-spacing was plotted against $\sin^2\psi$ for each of the samples (**Fig.1-5**). The calculation of the residual stress was automatically performed by the software of X'Pert Stress using the slopes "m", and the equation below:

$$\sigma = \frac{mE}{d0(1+\nu)} \quad (4)$$

Values of Young's modulus (E= 189.8 GPa) and Poisson's ratio (ν = 0.332) for the crystallographic plane (311) of nickel were used for the calculation. The positive value indicates tensile stress whereas the negative one expresses compressive stress. The results of residual stress are included in **Table 4** which shows that all samples have compressive stress (negative, from 39.3 MPa to 94.0 MPa).

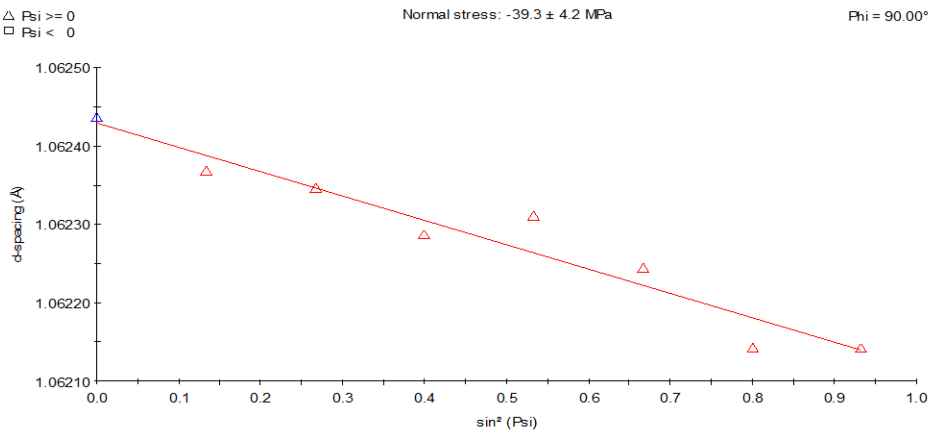


**FIG. 1. THE PLOT OF D-SPACING VS. SIN$^2\psi$ FOR THE COATING AT BATH TEMPERATURES OF 35°C**

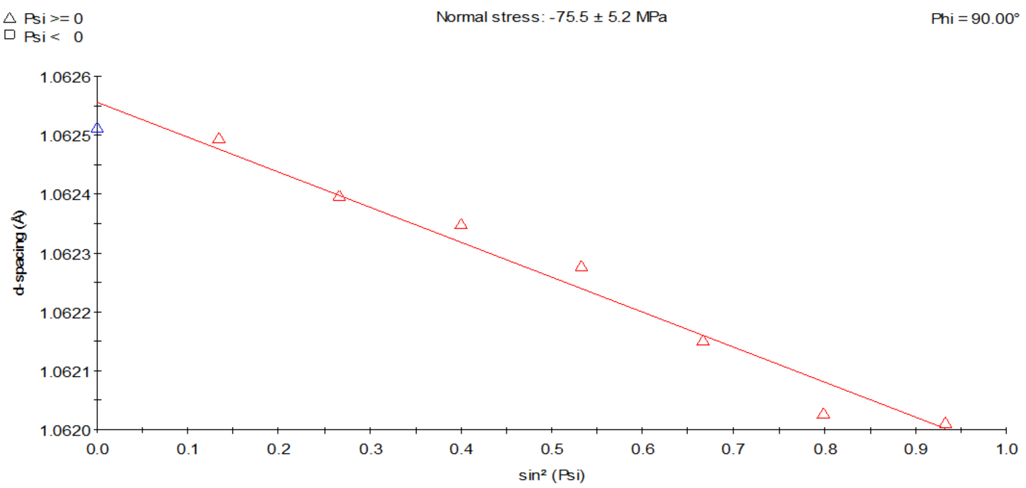


**FIG. 2. THE PLOT OF D-SPACING VS. SIN$^2\psi$ FOR THE COATING AT BATH TEMPERATURES OF 40°C**

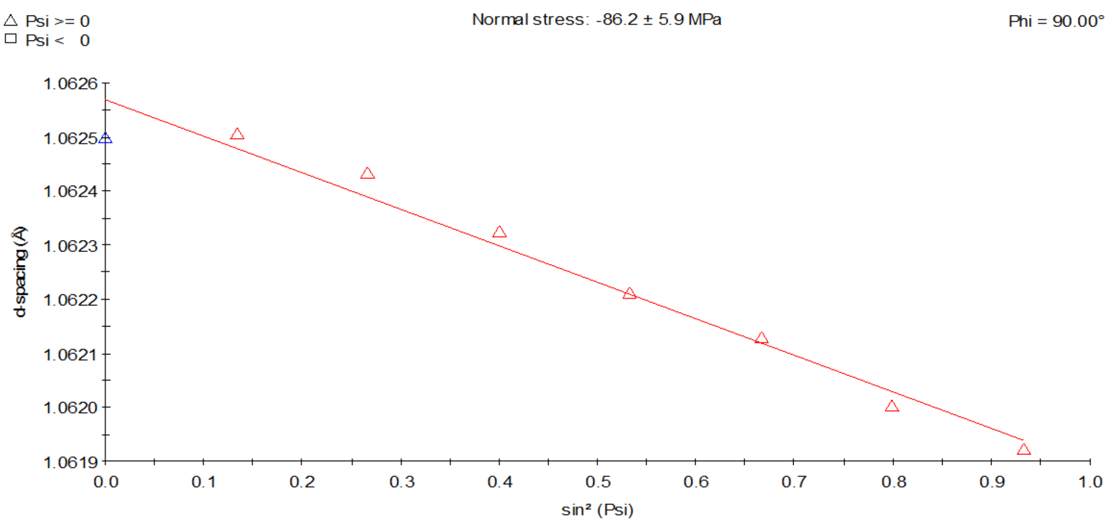


**FIG. 3. THE PLOT OF D-SPACING VS. SIN$^2\psi$ FOR THE COATING AT BATH TEMPERATURES OF 50°C**

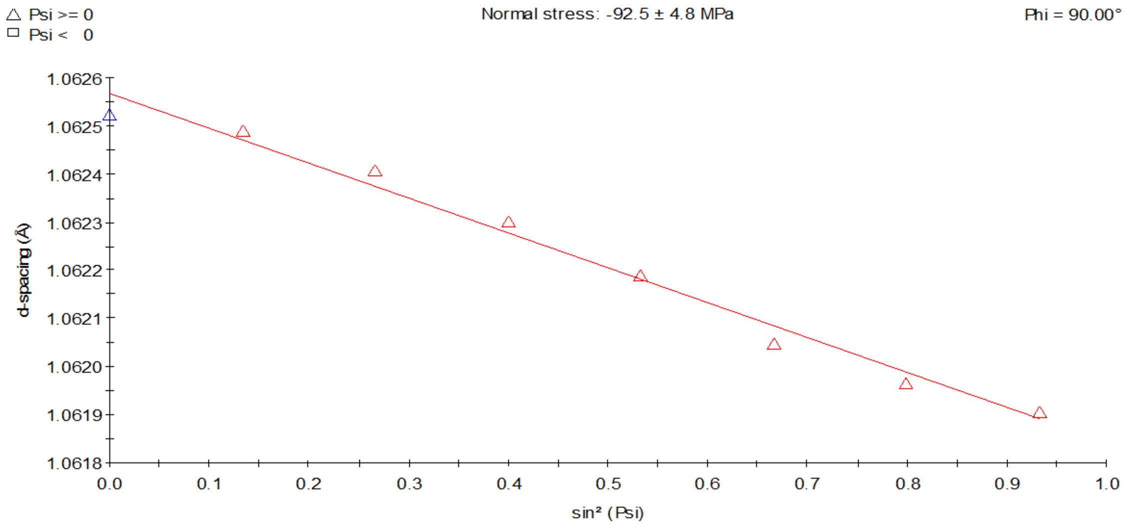


**FIG. 4. THE PLOT OF D-SPACING VS. SIN$^2\psi$ FOR THE COATING AT BATH TEMPERATURES OF 55°C**

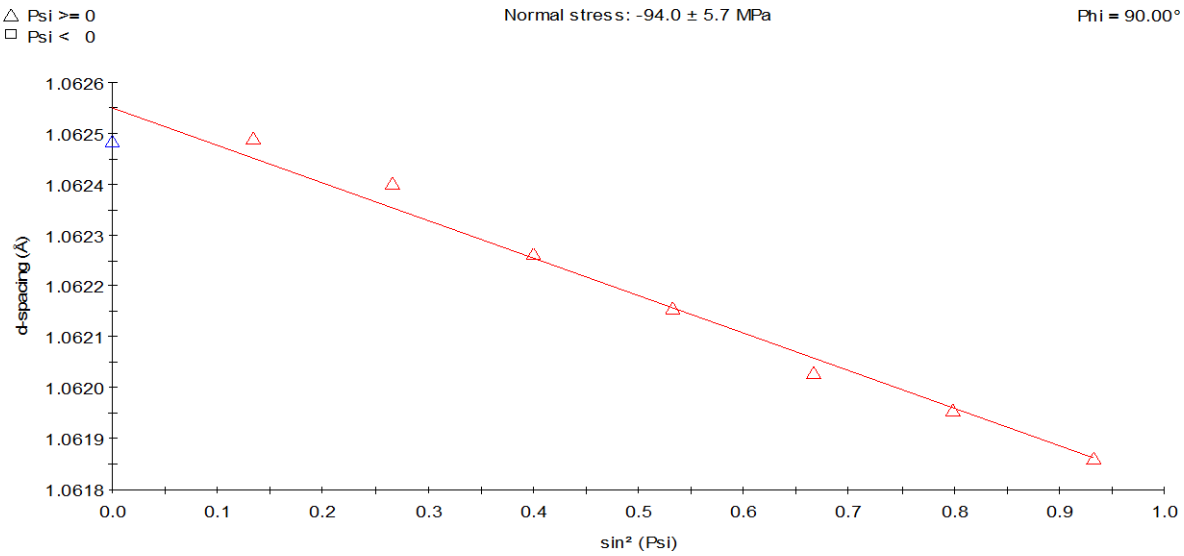


**FIG. 5. THE PLOT OF D-SPACING VS. SIN$^2\psi$ FOR THE COATING AT BATH TEMPERATURES OF 60°C**

### 3.4 Effect of Bath Temperature

As seen in **Fig 6a** and **Table 2**, nanocrystalline nickel deposits with an average crystallite size between 19 nm and 28 nm were obtained at all the investigated temperatures. The variation of the crystallite size of nickel coatings as a function of bath temperature has been observed in the present study. Figure 6a indicates that the crystallite size increase as the bath (plating) temperature increases from 35 °C to 60 °C, which confirmed the pattern presented by Dini [14]. It is generally expected that increasing the bath temperature results in an increase in the crystallite size of deposits as the over-potential decreases with increasing bath temperature and the energy of nucleus formation increases consequently. The energy of grain nucleus formation depends on the cathodic over-potential. The energy of nucleus formation decreases at large cathodic over-potential, and therefore the nucleus densities (the number of nucleus per surface area) increases and refinement of coating grains occurs. In other word, low temperature favors the formation of new nuclei rather than growth of existing grains. Therefore, when increasing the bath temperature decreases the cathodic over-potential, the crystallite size of deposits will enlarge. The theoretical model predicted by Rashidi and Amadeh [12] showed an exponential dependence of the grain size of deposits on bath temperature, which was confirmed by the experimental results only for 55 °C to 70 °C bath temperature range (**Fig.6b**).

A)

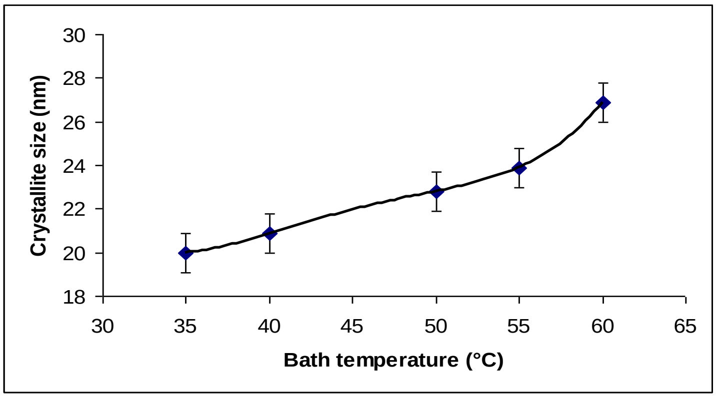


B)

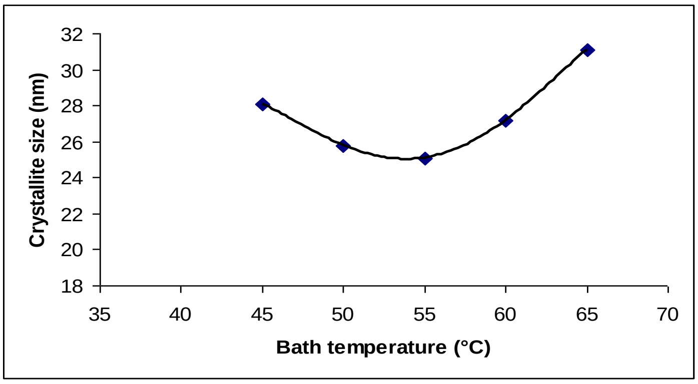


**FIG. 6. THE RELATIONSHIP BETWEEN THE TEMPERATURE OF THE ELECTROPLATING BATH AND THE CRYSTALLITE SIZE OF THE NANOCRYSTALLINE NI COATINGS. A) OUR RESULTS. B) THE RESULTS FROM THE REF. [12].**

As seen in **Fig. 7**, all diffraction peaks of (111) from nickel coatings and the reference nickel powder has the highest intensity. However, compared with the reference nickel powder, it is found that with increasing the bath temperature, the crystallographic plane of (100) (indicated by diffraction peak of (200)) gets more preferred orientation (bigger value of relative texture coefficient ($RTC_{(200)}$) (**Table 3** and **Fig. 8**).

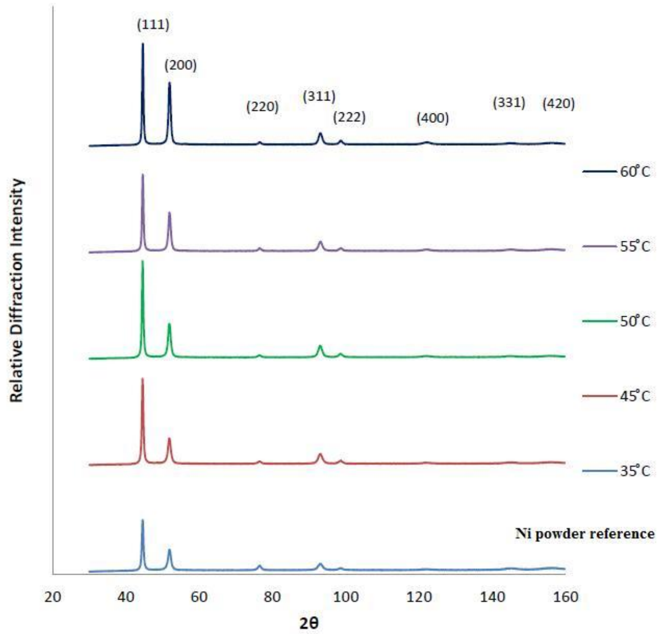


**FIG. 7. XRD PATTERNS OF NANOCRYSTALLINE NICKEL COATINGS AT DIFFERENT BATH TEMPERATURES AND NICKEL POWDER REFERENCE.**

N. A. Pangarov [18-20] suggested that the preferred orientation of the electrodeposited grain was decided by cathode over-potential. According to the calculation, electrodeposited nickel is most likely to form (111)-like texture at a low over potential as the {111} facets have the lowest energy. With the increase of over-potential, the preferential orientation is (200), and then (220) texture. According to Pangarov's statement, it is expected that with increasing the bath temperature, the over-potential will decrease and promote the preferred orientation of (111) rather than (200) and (220). Our results did not agree with Pangarov's statement. The reason probably is that some other factors such as crystallite size and deposited thickness also effect the preferred orientation. V. M. Kozlov et al [21] studied the influence of the thickness of fcc metals electrodeposited on an indifferent substrate on the formation of a preferred orientation of the crystalline grains. He concluded that the preferred orientation axis of the grains and the degree of perfection of the textures of electrodeposits depend on their thickness and not on the overvoltage value (in the case of potentiostatic conditions). He mentioned that by increasing the thickness of the deposits from 0.2 $\mu$m to 0.5 $\mu$m, a decrease in the degree of perfection of the [111] texture is observed. By further increasing such thickness, the preferred orientation axis changes and becomes the [100] axis in the case of Ni deposits.

A)

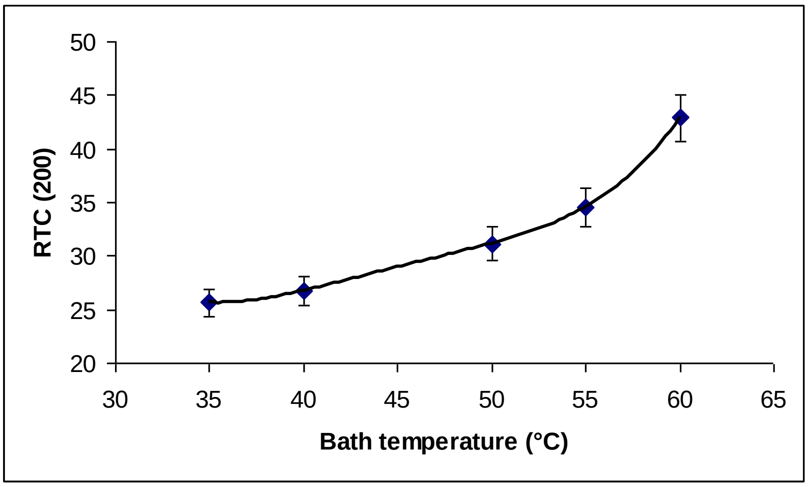


B)

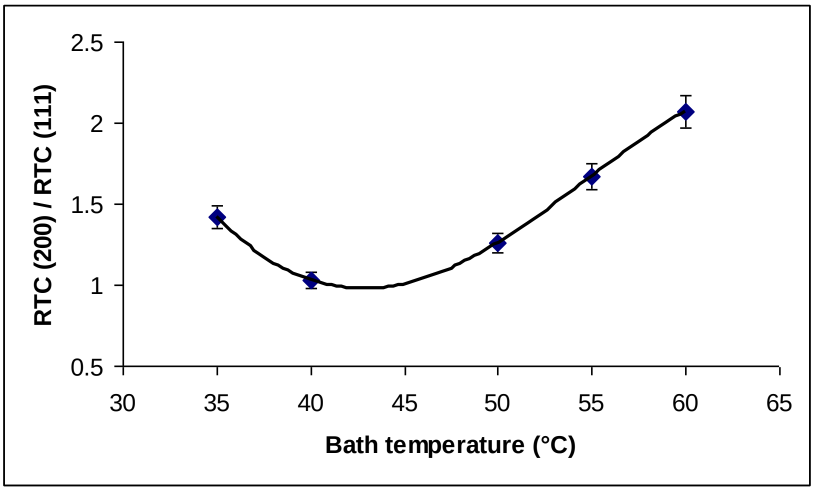


**FIG. 8. BATH TEMPERATURE VS. RELATIVE TEXTURE COEFFICIENT (RTC). A) BATH TEMPERATURE VS. RELATIVE TEXTURE COEFFICIENT (RTC) OF CRYSTALLOGRAPHIC PLANE OF (200). B) BATH TEMPERATURE VS. RATIO OF RTC (200) TO RTC (111).**

As seen in **Fig. 9**, it is noted that with increasing the bath temperature, the compressive residual stress (negative value) of nickel coatings increases as the higher temperature enlarges the thermal expansion coefficient mismatch between the substrate and nickel coating. Additionally, this might partly be due to the enlargement of the crystallites size that is accompanied with the increase in temperature [22]. Therefore, moderate temperature is recommended to apply in the electrodeposition process of nanocrystalline nickel coatings since moderate compressive stress is beneficial for increasing the adhesion of the coating and enhancing coating integrity. It was reported that the wear-resistant coatings are working better under the condition of relatively high compressive stresses, which prevent from the development of fatigue cracks [23, 24].

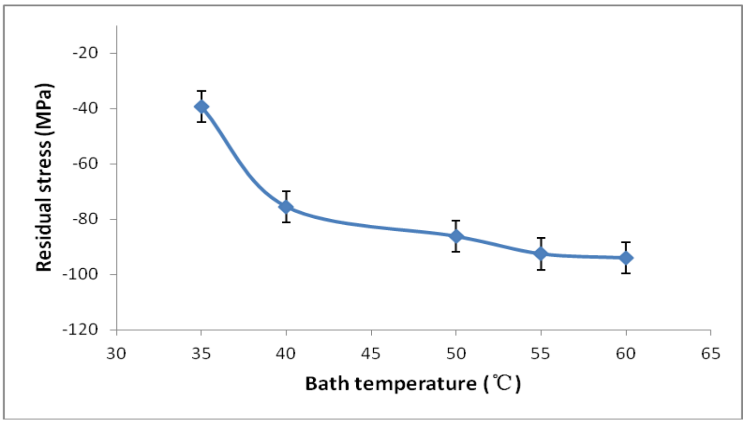


**FIG. 9. BATH TEMPERATURE VS. COMPRESSIVE RESIDUAL STRESS**

## IV. CONCLUSION

Based on the experimental results, it is found that with increasing temperature, the average crystallite size, relative texture coefficient of crystallographic plane (200) (same direction as (100)), and compressive residual stress increase. Therefore, it can be concluded that moderately increasing the temperature (up to about 60 °C) in the process of nanocrystalline nickel coating production will promote the preferred orientation of crystallographic plane (100) and the compressive residual stress, which enhances nickel crystal compaction, coating adhesion, and coating integrity.

## REFERENCES

[1] S. C. Tjong, H. Chen, Nanocrystalline materials and coatings, Mater. Sci. Eng., 2004. R 45: p. 1-88.
[2] L. Wang, Y. Gao, T. Xu, Q. Xue, A comparative study on the tribological behavior of nanocrystalline nickel and cobalt coatings correlated with grain size and phase structure, Mater. Chem. Phys., 2006. 99: p. 96-103.
[3] N. S. Qu, D. Zhu, K. C. Chan, W. N. Lei, Pulse electrodeposition of nanocrystalline nickel using ultra narrow pulse width and high peak current density, Surf. Coat. Technol., 2003. 168: p. 123-128.
[4] U. Erb, Electrodeposited nanocrystals: Synthesis, structure, properties and future applications, Can. Metall., 1995. Q 34: p. 275-280.
[5] F. Ebrahimi, Z. Ahmed, The effect of current density on properties of electrodeposited nanocrystalline nickel, J. Appl. Electrochem., 2003. 33: p. 733-739.
[6] D. Bera, S. C. Kuiry, S. Seal, Synthesis of nanostructured materials using template-assisted electrodeposition, JOM, 2004. 56: p. 49-53.
[7] H. Natter, R. Hempelmann, Tailor-made nanomaterials designed by electrochemical methods, Electrochim. Acta, 2003. 49: p. 51-61.
[8] H. Natter, R. Hempelmann, Nanocrystalline Metals Prepared by Electrodeposition, J. Phys Chem., 2008. 222: p. 319-354.
[9] R. Sen, S. Das, K. Das, The effect of bath temperature on the crystallite size and microstructure of Ni–CeO2 nanocomposite, Mater. Charact., 2011. 62: p. 257-262.
[10] R. Hempelmann, H. Natter, Nanocrystalline Copper by Pulsed Electrodeposition: The Effects of Organic Additives, Bath Temperature, and pH, J. Phys. Chem., 1996. 100: p. 19525-19532.
[11] Y. Tan, K. Y. Lim, Understanding and improving the uniformity of electrodeposition, Surf. Coat. Technol., 2003. 167: p. 255-262.
[12] A. M. Rashidi, A. Amadeh, The effect of saccharin addition and bath temperature on the grain size of nanocrystalline nickel coatings, Surf. Coat. Technol., 2009. 204: p. 353-358.
[13] A. M. Rashidi, A. R. Eivani, A. Amadeh, Application of artificial neural networks to predict the grain size of nano-crystalline nickel coatings, Compu. Mater. Sci., 2009. 45: p. 499-504.
[14] J. W. Dini, Electrodeposition: The Materials Science of Coatings and Substrates, Noyes Publications, New Jersey, 1993. P. 141-142.
[15] P. Scherrer, Bestimmung der Grösse und der inneren Struktur von Kolloidteilchen mittels Röntgensrahlen [Determination of the size and internal structure of colloidal particles using X-rays], Nachr. Ges. Wiss. Gòttingen, Math Phys., 1918. Kl. 26: p. 98-100.
[16] G. C. Ye, D. N. Lee, Orientation and microstructure of dull nickel electrodeposits, Plat. Surf. Finish., 1981. 68: p. 60-64.
[17] M. E. Hilley, Residual Stress Measurement by X-Ray Diffraction, SAE J784a, Society of Automotive Engineers, New York, 1971. P. 21-24.
[18] N. A. Pangarov, The crystal orientation of electrodeposited metals, Electrochim. Acta, 1962. 7: p. 139-146.
[19] N. A. Pangarov, Preferred orientations in electro-deposited metals, J. Electroanal Chem., 1965. 9: p. 70-85.
[20] N. A. Pangarov, V. Velinov, The orientation of silver nuclei on a platinum substrate, Electrochim. Acta, 1966. 11: p. 1753-1758.
[21] V. M. Kozlov, L. P. Bicelli, Texture formation of electrodeposited fcc metals, Mater. Chem. Phys., 2002. 77: p. 289-293.

[22] F. Czerwinski, Grain Size-Internal Stress Relationship in Iron-Nickel Alloy Electrodeposits, J.Electrochem.Soc., 1996. 143: p. 3327-3332.

[23] A. A. Solov'ev, N. S. Sochugov, K. V. Oskomov, Influence of Deposition Parameters on Properties of Magnetron Sputtered Ag Films The Phys. Of Mate. And Metallo., 2010. 109 (2): p. 111-115.

[24] Q. Xu, Y. Qiao, H. Liu, W. Meng, Electrodeposition and characterizations of nickel coatings on the carbon–polythene composite, J Appl Electrochem., 2009. 39: p. 2513-2519.